TWO DIMENSIONAL STUDY OF HYDRAULIC FRACTURING CRITERIA IN COHESIVE SOILS

EIJI YANAGISAWA[i] and ALI KOMAK PANAH[ii]

ABSTRACT

Based on the shear failure mechanism, hydraulic fracturing criteria are extended to three dimensional stress state. According to the situation of the directions of borehole and major principal stress axes, three equations can be derived for three dimensional hydraulic fracturing problems. By comparing these equations, a single criterion is selected for hydraulic fracturing pressure in cohesive soils. The criterion is a function of maximum principal stress, minimum principal stress and soil parameters in UU conditions. The equation indicates that with any increase in maximum principal stress, hydraulic fracturing pressure decreases. In order to prove the integrity of the criteria, laboratory tests are performed on compacted cubical specimens using true a triaxial apparatus. The shape and direction of fractures are determined by injecting colored water after fracture initiation. It is found that the direction of fractures are perpendicular to the σ_1 plane.

Key words: cohesive soil, failure, grouting, laboratory test, pore pressure (IGC: K2/D6)

INTRODUCTION

The concept of generating fractures in soil or rock by liquids, has been recognized in connection with pressure grouting, in field permeability testing, in-situ pressure measurement, oil industry and dam engineering. The possibility, however, of cracks being formed in zoned earth dams due to hydraulic fracturing has become a controversial issue in the geotechnical literature, especially after the failure of Teton Dam in United States on June 5, 1976 when the reservoir filling was nearly complete (Independent Panel of Experts and Another of Top Dam Designers in Federal Agencies, 1977).

Excessive leakage attributable to hydraulic fracturing in embankment dams has been reported at Hyttejuvet Dam in Norway (Kjaernsli and Torblaa, 1968), low-level flood control dams in Oklahoma and Mississippi (Sherard, 1985), Stockton Creek Dam, Wister Dam, Yard's Creek Upper Reservoir Dam (Sherard, 1985), Balderhead Dam (Vaughan et al., 1970), and Teton Dam (Independent Panel of Experts and Another of Top Dam Designers in Federal Agencies, 1977). In each of these cases, although it has not been possible to prove by direct observation that hydraulic fracturing has been responsible for excessive leakage or failure, an overwhelming amount of evidence has been accumulated to indicate that this could, in fact, have occurred. Other mechanisms have also been proposed in many of these cases, and it is important to recognize that hydraulic fracturing is by no means the only possible explanation of the leakage which has occurred. Nevertheless, it is a realistic possibility in most of the cases cited (Sherard, 1986).

A number of investigators have performed in-situ hydraulic fracturing tests (Bjerrum and Andersen, 1972; Bjerrum et al., 1974; Independent Panel to Review Cause of Teton Dam Failure, 1976; Vaughan, 1971) by increasing the water pressure in either open boreholes or piezometers. A review of all these tests shows clearly that hydraulic fracturing can readily be induced in boreholes.

Laboratory investigations for hydraulic fracturing in soils were performed by Jaworski, et al. (1981), Fukushima (1986), Mori and Tamura (1987) and Komak Panah and Yanagisawa (1989). In all the cases it was found that hydraulic fracturing pressure in a hollow cylindrical specimen of cohesive soils can be written in the linear form of:

$$P_f = m\sigma_h + n \tag{1}$$

where P_f: hydraulic fracturing pressure, σ_h: confining pressure, m and n are related to material constants.

Equation (1) can be applied only to some special geotechnical problems. These problems are limited to in situ permeability tests, in situ pressure measurements and pressure grouting which are usually executed in the

[i] Professor, Department of Civil Engineering, Tohoku University, Sendai, Miyagi.
[ii] Former Graduate Student, ditto.
Manuscript was received for review on April 8, 1991.
Written discussions on this paper should be submitted before October 1, 1994 to the Japanese Society of Soil Mechanics and Foundation Engineering, Sugayama Bldg. 4 F, Kanda Awaji-cho 2-23, Chiyoda-ku, Tokyo 101, Japan. Upon request the closing date may be extended one month.

natural ground in which a borehole is drilled to apply injection pressure. The horizontal ground pressure is assumed approximately to be uniform around the borehole and the stress state is similar to a hollow cylindrical specimen. The criteria in which the effect of maximum principal stress is absent, can not be satisfactorily applied to three dimensional problems in real structures such as earth dams.

In this study the hydraulic fracturing criteria were extended theoretically to three dimensional stress state based on the theory of elasticity. According to the situation of borehole and the direction of principal stresses, three equations were computed for three dimensional problems. By comparing these equations, a single criterion was found for hydraulic fracturing in cohesive soils. In order to prove the integrity of the criteria, laboratory tests were performed on compacted cubical specimens using a true triaxial apparatus.

HYDRAULIC FRACTURING CRITERIA IN HOLLOW CYLINDRICAL SPECIMEN

The earlier hydraulic fracturing criteria in hollow cylindrical specimens were proposed by Komak Panah and Yanagisawa (1989). Considering a sample section as a thick cylinder (Fig. 1) and assuming homogeneous, isotropic and elastic behavior of material, effective radial and circumferential stresses near the borehole of a hollow cylindrical specimen become:

$$\sigma_r' = \sigma_r - u \tag{2}$$

$$\sigma_\theta' = \frac{2\sigma_h b^2 - P_f(b^2+a^2)}{b^2-a^2} - u \tag{3}$$

where σ_r': effective radial stress, σ_θ': effective circumferential stress, P_f: hydraulic fracturing'pressure, σ_h: confining pressure, u: pore water pressure near the borehole, a and b: internal and external radii of specimen and positive stresses are compression.

Throughout the test process, seepage of water into the soil sample was expected, so that the pore water pressure around the borehole becomes approximately equal to the internal water pressure. Thus effective radial stresses around the borehole from Eq. (2) are equal to zero. On the other hand, the effective circumferential stress around the borehole is compression if the internal pressure ranging from zero to a value less than the confining pressure. The condition in which effective circumferential stress around the borehole becomes zero is the beginning of the hydraulic fracturing tests where P_f is equal to the confining pressure σ_h. From this condition any excess increase of internal water pressure will result in tensile effective circumferential stress. This will cause the hydraulic fracturing, which is assumed to be initiated by the shear failure due to the radial stress and the circumferencial stress near the borehole. When shear failure is assumed it would be known from the zero effective stress state at the $P_f=\sigma_h$ condition that shear failure takes place in unconsolidated undrained conditions near the borehole (Komak Panah and Yanagisawa, 1989). Therefore stress analysis should be accomplished in terms of total stresses.

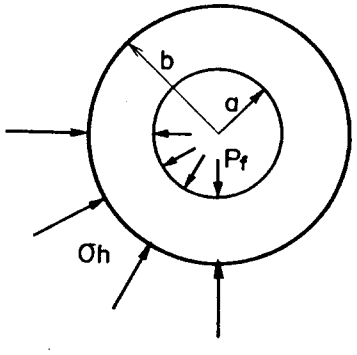

Fig. 1. Cylindrical sample section

Total radial and circumferential stresses near the borehole can be written in the forms:

$$\sigma_r = P_f \tag{4}$$

$$\sigma_\theta = \frac{2\sigma_h b^2 - p_f(b^2+a^2)}{b^2-a^2} \tag{5}$$

where positive stresses are compression. In the hydraulic fracturing tests, stress state near the borehole becomes $\sigma_r > \sigma_\theta$, and Mohr-Coulomb criterion in UU conditions is written in the form:

$$(\sigma_r - \sigma_\theta) = (\sigma_r + \sigma_\theta)\sin\phi_u + 2c_u\cos\phi_u \tag{6}$$

where

ϕ_u: angle of internal friction. (UU condition)
c_u: cohesion of soil. (UU condition).

Substituting Eq. (4) and Eq. (5) into Eq. (6), a following expression was obtained for hydraulic fracturing pressure:

$$P_f = \frac{b^2(1+\sin\phi_u)}{b^2+a^2\sin\phi_u}\sigma_h + \frac{c_u(b^2-a^2)\cos\phi_u}{b^2+a^2\sin\phi_u}. \tag{7}$$

Equation (7) was examined in compacted cohesive soils (Komak Panah and Yanagisawa, 1989) and fairly good agreements were found between theoretical and experimental results (Fig. 2).

If the external radius of specimen is considered to be large enough, Eq. (7) can be simplified to the following form:

$$P_f = (1+\sin\phi_u)\sigma_h + 2c_u\cos\phi_u. \tag{8}$$

This equation can be applied for the estimation of the pressure to initiate the hydraulic fracturing of soils near a small borehole in a large cylindrical specimen.

Bjerrum et al. (1974) proposed a hydraulic fracturing criterion by taking into account vertical stress and deformation of soils around the borehole. Therefore the equation derived is expressed in terms of dimension of specimen, the strength parameter and elastic modulus of

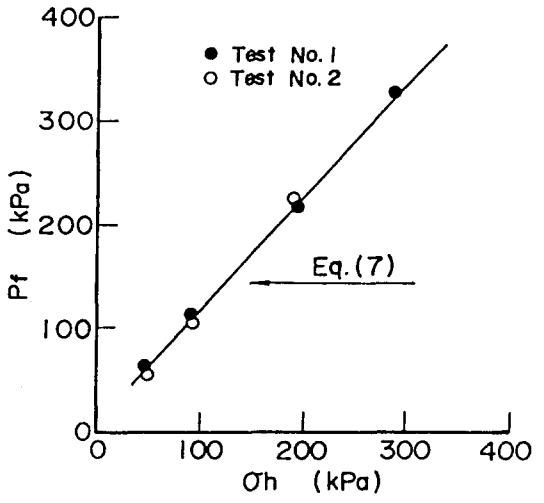

Fig. 2. Comparison between Eq. (7) and experimental hydraulic fracturing pressures in Aoba Yama Loam. (Komak Panah and Yanagisawa, 1989)

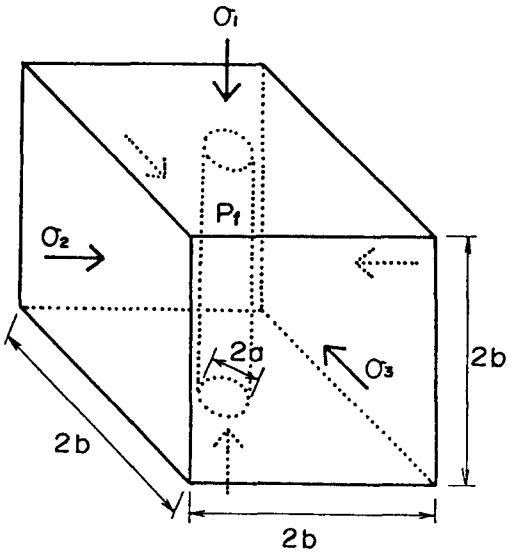

Fig. 3. Cubical specimen with a small borehole in the direction of maximum principal stress

soils. In this paper, however, the effect of axial stress is neglected to avoid the complexity, and the problem is simplified to the two dimensional plane stress state, then the elastic modulus of soils does not appear in the fracturing criteria.

STRESS ANALYSIS OF CUBICAL SPECIMEN

Let us consider a cubical specimen with a small borehole in the direction of the maximum principal stress as shown in Fig. 3. Assuming linear elastic behavior of material and neglecting the effect of σ_1 in the horizontal direction, this can be divided into three different stress conditions. Consider the stress states of a plate with a small hole, subjected to a principal stress σ_3, another principal stress σ_2 and an internal pressure P_f inside the hole, respectively. By analyzing each problem and superimposing the results, stress components around the borehole can be obtained.

From well established elastic solutions Timoshenko and Goodier (1951) of stress distribution around a hole in an infinite plate subjected to an uniform compressive stress at an infinite distance, we find:

$$\sigma_r=\frac{\sigma_3}{2}\left(1-\frac{a^2}{r^2}\right)+\frac{\sigma_3}{2}\left(1+\frac{3a^4}{r^4}-\frac{4a^2}{r^2}\right)\cos 2\theta \tag{9}$$

$$\sigma_\theta=\frac{\sigma_3}{3}\left(1+\frac{a^2}{r^2}\right)-\frac{\sigma_3}{2}\left(1+\frac{3a^4}{r^4}\right)\cos 2\theta \tag{10}$$

$$\tau_{r\theta}=-\frac{\sigma_3}{2}\left(1-\frac{3a^4}{r^4}+\frac{4a^2}{r^2}\right)\sin 2\theta. \tag{11}$$

Thus the stresses near the borehole ($r=a$) will be given as:

$$\sigma_{r1}=0 \tag{12}$$

$$\sigma_{\theta 1}=\sigma_3(1-2\cos 2\theta) \tag{13}$$

$$\tau_{r\theta 1}=0. \tag{14}$$

Replacing σ_3 and θ in Eq. (13) by σ_2 and $(\pi/2-\theta)$, we can get stresses near the borehole in the case of uniform compressive principal stress σ_2:

$$\sigma_{r2}=0 \tag{15}$$

$$\sigma_{\theta 2}=\sigma_2(1+2\cos 2\theta) \tag{16}$$

$$\tau_{r\theta 2}=0. \tag{17}$$

For the case of application of the internal pressure P_f from inside the hole, assuming a large cylindrical specimen and analyzing as a thick cylinder, it gives:

$$\sigma_{r3}=P_f \tag{18}$$

$$\sigma_{\theta 3}=-P_f \tag{19}$$

$$\tau_{r\theta 3}=0. \tag{20}$$

Adding the values of the stresses in these three cases together, we can get the stress components near the borehole in the considered cubical specimen in which the internal pressure P_f is applied into the borehole:

$$\sigma_r=P_f \tag{21}$$

$$\sigma_\theta=\sigma_3(1-2\cos 2\theta)+\sigma_2(1+2\cos 2\theta)+P_f \tag{22}$$

$$\tau_{r\theta}=0. \tag{23}$$

Assumed that hydraulic fracturing is initiated by shear failure, then hydraulic fracturing criteria can be calculated by substituting Eqs. (21) and (22) into the Mohr-Coulomb criterion in the unconsolidated undrained condition. The resulting equation becomes:

$$P_f=0.5(\sigma_3+\sigma_2)(1+\sin\phi_u)-(\sigma_3-\sigma_2)(1+\sin\phi_u)\cos 2\theta + c_u\cos\phi_u. \tag{24}$$

The critical value of the hydraulic fracturing pressure is the minimum of Eq. (24) with respect to θ. Therefore Eq. (24) gives not only hydraulic fracturing criteria, but also the direction of the fracture. Because of the condition of $\sigma_2 > \sigma_3$, the minimum value of Eq. (24) will appear when $\theta = \pi/2$. In this condition hydraulic fracturing criteria becomes:

$$P_f = (1.5\sigma_3 - 0.5\sigma_2)(1 + \sin \phi_u) + 2c_u \cos \phi_u. \quad (25)$$

Substituting $\sigma_2 = \sigma_3$ in Eq. (25), the equation reduces to the same expression of hydraulic fracturing criteria which was found by conventional triaxial hydraulic fracturing for hollow cylindrical specimens (Eq. (8)). An important point of Eq. (25) is the effect of σ_2 in the hydraulic fracturing pressure in which by increasing the intermediate stress hydraulic fracturing pressure will decrease.

If the borehole is made in the direction of σ_2 or σ_3 Eq. (27) can be written in following forms:

$$P_f = (1.5\sigma_3 - 0.5\sigma_1)(1 + \sin \phi_u) + 2c_u \cos \phi_u \quad (26)$$

$$P_f = (1.5\sigma_2 - 0.5\sigma_1)(1 + \sin \phi_u) + 2c_u \cos \phi_u. \quad (27)$$

In practice in which the stress condition can be assumed as $\sigma_1 > \sigma_2 > \sigma_3$, the maximum hydraulic fracturing pressure should be calculated from Eq. (26) rather than Eq. (25) or (27). Therefore Eq. (26) can be represented as a hydraulic fracturing criterion in in-situ conditions.

One way of the examination of the validity of Eq. (26), can be generally made by equating hydraulic fracturing pressure to confining pressure. It has been known that when unconsolidated undrained triaxial tests are performed on a fully saturated soil sample, ϕ_u becomes zero, whereas ϕ_u appears when the sample is partially saturated. Therefore considering $P_f = \sigma_3$, $\phi_u = 0$ and substituting these conditions into Eq. (26) gives:

$$\sigma_1 = \sigma_3 + 2c_u = \sigma_3 + q_u. \quad (28)$$

Equation (28) coincides with the well known failure condition of clay in unconsolidated undrained conditions. This explanation indicates the integrity of the Eq. (26).

LABORATORY INVESTIGATIONS

The investigations were performed on a compacted cohesive silty clay (Aoba Yama Loam). After pulverization of air dried soil sample, it was sieved by a sieve of 0.42 mm opening. The properties of the soil sample are as follow:

$\phi' = 29°$, LL = 49.82%, PL = 25.54%, PI = 24.28,
Gs = 2.71, clay = 43%, silt = 41%, sand = 16%,
optimum water content = 36%.

Also from a series of unconsolidated undrained triaxial tests, $\phi_u = 6.5°$ and $c_u = 10.8$ kPa were found for compacted specimens with the same density.

Cubical specimens with the side length of 10 cm and a borehole in σ_1 direction (axial direction) with the diameter of 2 cm, were used for hydraulic fracturing tests. The soil with optimum water content was compacted in five layers by the static loading of about 294 kPa.

Test Apparatus

Figure 4 shows the schematic diagram of the hydraulic fracturing apparatus. This is a true triaxial apparatus with some changings in the bottom, upper platen and connections. The lateral pressures are applied by water pressure onto the side planes of the cell through rubber membranes. Figure 5 shows some details of the cubical cell which was designed for these special experiments. The internal pressure and both lateral pressures as well as the axial pressure can be controlled separately. Also the inflow water to the borehole is measured by flow-meter, therefore the flow rate during the test can be obtained, and finally permeability of the soil can be determined. Through the test procedure sudden increase of the flow indicates the occurrence of the hydraulic fracturing in the specimen.

Three series of tests were performed in this study under different lateral and axial pressures. These are summarized in Table 1.

Test Procedure

Through all the series of the tests, drain paper was provided to keep the pore water pressure at the sample surface equivalent to the atmospheric pressure. By opening or closing some of the valves as shown in Fig. 4, a process of the tests divided into several stages as follow:

Stage (1)—The specimen was placed in the hydraulic fracturing test apparatus. To prevent the leakage from the top and bottom of the sample, grease was spread on the end of platens. Drained paper was attached to the sample surface to increase the capacity of the flow through the sample. Inner part of the specimen was filled by washed and graded sands, which was graded between 0.84 mm and 0.25 mm. Finally the upper part of the apparatus was fixed.

Stage (2)—To prevent the leakage from the top and the bottom of the specimen, a slight axial pressure (9.8 kPa) was applied.

Stage (3)—By flushing the sand column in the specimen from the bottom, remained air bubbles between the sample and sand were expelled.

Stage (4)—With the same rate of pressure, axial pressure, lateral pressure and internal water pressure were applied simultaneously until they reach the minor principal stress state. Then the major and intermediate stresses were increased until they reach a certain stress state of the test.

Stage (5)—Under constant, axial and lateral pressures, the internal water pressure was increased until the fracture occurred in the sample. The rate of water pressure increase was kept constant for all the tests namely 4.9 kPa/min. This pressurizing rate was decided from the permeability coefficient of soil sample.

Stage (6)—To clarify the direction of fractures, after fracturing of the specimen, the water colored by

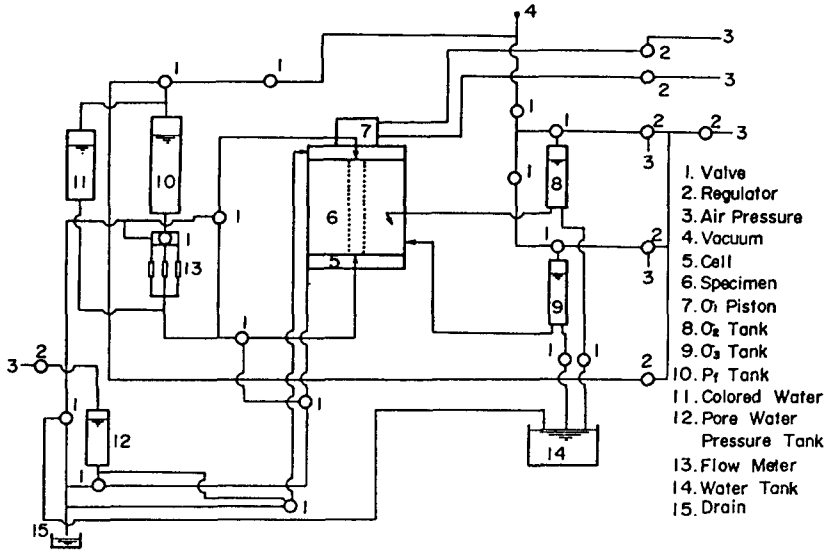

Fig. 4. Schematic diagram of the hydraulic fracturing apparatus

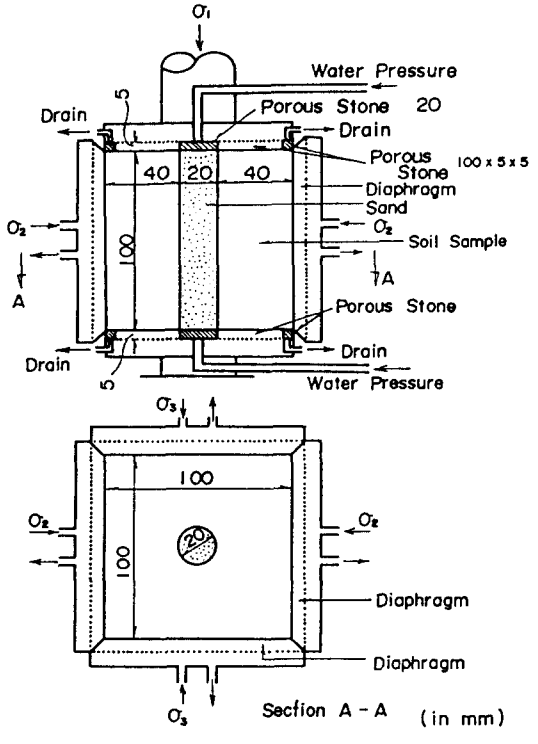

Fig. 5. Details of the cell in hydraulic fracturing apparatus

Rhodamine B was injected into the borehole with the same fracturing pressure. The shape and direction of fractures were determined by observing the state of colored water penetration after cutting down the specimen.

Table 1. Axial and lateral applied stresses in different series of the tests

Test series	Maximum principal stress kPa	Minimum principal stress kPa	Intermediate principal stress kPa
1	49	29	29
	69	49	49
	88	69	69
	118	98	98
2	49	29	34
	49	29	39
	49	29	44
	49	29	49
3	69	49	54
	69	49	59
	69	49	64
	69	49	69

Limitation of the Tests

It is clear that at the beginning of each test, when the internal water pressure becomes equal to the isotropic lateral pressure ($\sigma_2=\sigma_3$), pore water pressure near the borehole will reach the same circumferential stress of borehole due to the penetration of water into the soil sample. According to this value of the pore water pressure, the effective stresses around the borehole drop to zero and the condition becomes the unconsolidated undrained condition. Thus a portion around the borehole may fail if a higher axial pressure is applied. The failure is a kind of unconsolidated undrained shear failure. Therefore in order to perform a safe hydraulic fracturing test, it is necessary to keep the applied stresses in the following limits:

$$\sigma_3 \leq \sigma_2 \leq \sigma_1 \leq \sigma_3 + q_u. \tag{29}$$

Throughout the laboratory studies, the tests were performed under the limitation of inequality (29).

Another limitation of the tests which was applied in tests, is the value of minor principal stress. When higher pressures are applied, corresponding internal water pressures to fracture will increase and the velocity of the flow through the sample also increases. As a stress state in the corners of the specimen is far smaller than the center (because of the boundary conditions of loading membranes), even in the case of using special drain paper, suddenly piping occurs through the corners of the specimen. For this reason the tests were performed under σ_3 lower than 98 kPa.

Test Results

A sudden increase of inflow at a water pressure inside the sand column indicates the hydraulic fracturing occurrence in the sample. This increase is due to the penetration of water into the fractures and internal water pressure at this moment is equivalent to the maximum hydraulic fracturing pressure. Figure 6 shows a typical curve of flow rate versus internal water pressure.

In order to compare the hydraulic fracturing equation obtained from the hollow cylindrical specimen with experimental results of cubical hydraulic fracturing tests, the first series of the tests were performed in the condition of lateral isotropic pressure ($\sigma_2 = \sigma_3$). Figure 7 shows the comparison of the hydraulic fracturing criteria obtained from Eq. (8) and experimental results. Good agreement indicates that proposed criteria can be applied to a cubical shape of specimen. Note that the substituted unconsolidated undrained strength parameters of soil in the criteria, were found by performing triaxial tests on the soil sample.

The second series and third series of the tests were performed with different stress states. In all these tests axial stress σ_1 was kept as the maximum. Minimum principal stress σ_3 was kept constant while the value of σ_2 changed from test to test. The values of σ_3 in second series and third series were 29 and 49 kPa respectively. Comparison

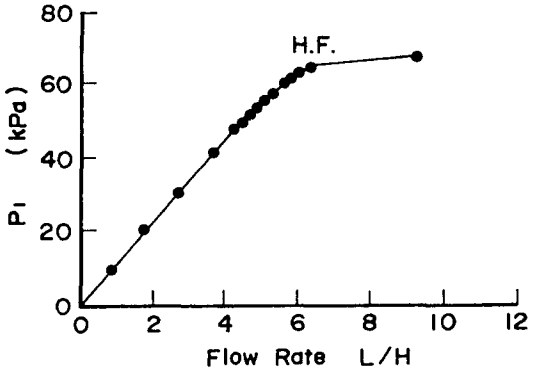

Fig. 6. Typical curve of flow rate versus internal water pressure

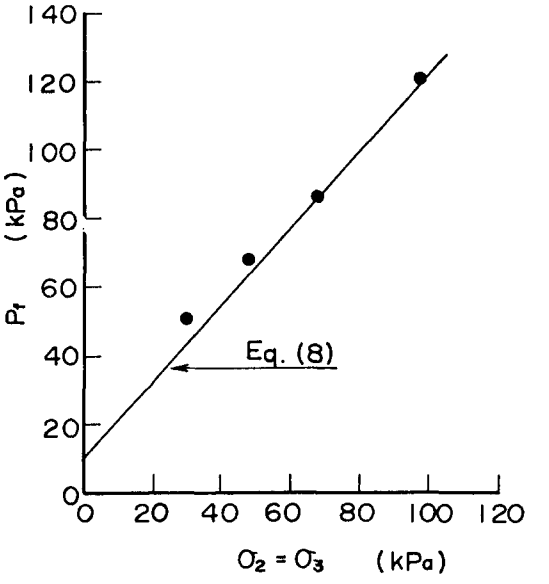

Fig. 7. Comparison of the hydraulic fracturing criteria and test results of first series

of the test results with Eq. (25), in which the quantities of ϕ_u and c_u are taken as 6.5° and 10.8 kPa respectively, are shown in Figs. 8 and 9. Comparatively good agreement can be seen in the figures. A little difference of theoretical hydraulic fracturing criterion from experimental results might stem from the assumption of infinity in the theoretical stress analysis and from effects of σ_1 to the stress state near the borehole. As we mentioned before, the calculations accomplished in infinite media. Also the distribution of uniform pressure near the corners of the specimen is assumed in the theoretical consideration. In the actual test specimen, however, a uniform distribution of loading pressure cannot be obtained because of the complexity of the equipment. A slight difference in the

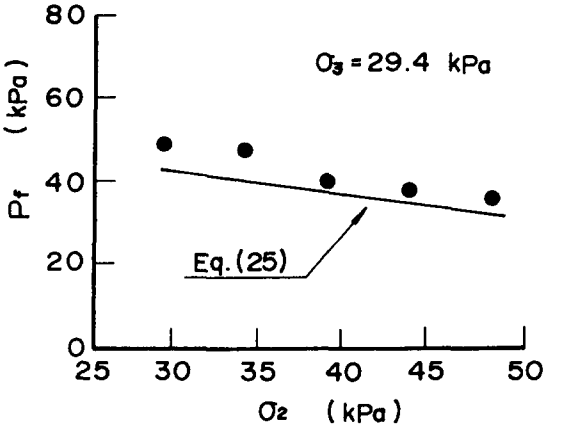

Fig. 8. Comparison of the hydraulic fracturing criteria and test results of the second series

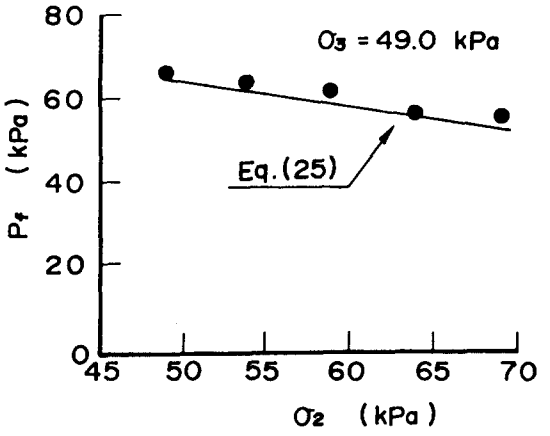

Fig. 9. Comparison of the hydraulic fracturing criteria and test results of the third series

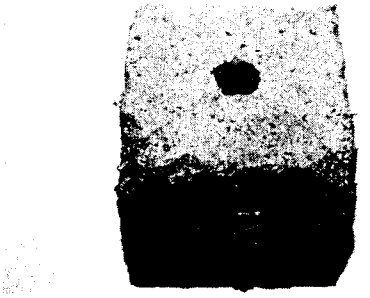

Fig. 10. Photograph of a specimen after fracturing. (First series)

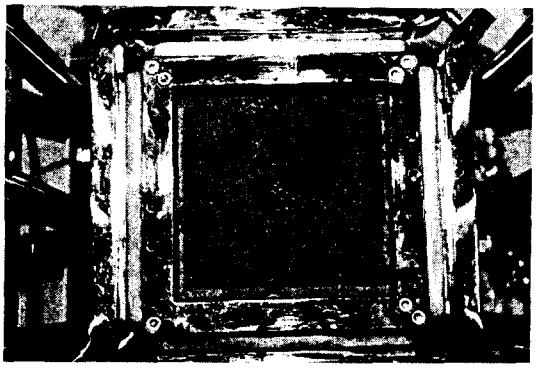

Fig. 11. Photograph of a specimen after fracturing. (Second series)

stress distribution may cause some change in the fracturing pressure. Existence of σ_1 will probably affect also on the shear strength of soil. Stress states near the borehole in the specimen are somehow similar to the plane strain condition and the shear strength in σ_1 plane will be obviously affected by the σ_1 stress. Further detailed studies are needed for the explanation of the difference between the test results and the theoretical ones.

DIRECTION OF FRACTURES

Referring to Eq. (24), in the first series of the tests ($\sigma_2=\sigma_3$), the hydraulic fracturing pressure is independent upon the direction of applied stresses (θ angle) and the fracture should occur in any direction but the test results show that the direction of fracture is always in a diagonal direction of specimen. A photograph of a specimen after taking out from the apparatus is shown in Fig. 10. This means that in a finite specimen in which an isotropic lateral pressure is applied, it is difficult to get a uniform stress around the borehole and the circumferential stress on the borehole boundary of the side direction is a little greater than that of diagonal direction. Probably this also happens on the second series of the tests in which cracks must initiate on the side direction (based on Eq. (24)). Therefore the actual circumferential stress is a little greater on the side direction of a finite specimen and experimental hydraulic fracturing pressure in the second series and third series should be a little larger than one obtained from Eq. (25).

On the second series and third series of the tests the directions of the fractures were perpendicular to the minor principal stress plane. A photograph of a specimen is shown in Fig. 11.

In the case of tests in which the difference between σ_2 and σ_3 was small enough, namely $\sigma_2=\sigma_3+4.9$ kPa, the fracture near the borehole occurred perpendicular to the σ_2 plane but in a small distance from the borehole it deviated to the corner direction. This clearly shows the effect of boundary conditions and at the same time suggests that the plastic region around the borehole is very thin. Therefore it should be noted that the equations obtained can be applied only for the initiation of the hydraulic fracturing.

EFFECT OF BOREHOLE SHAPE

In order to investigate the effect of borehole shape some tests were performed with the similar condition to the first series of the tests using samples in which a small notch had been made along the borehole. Figure 12 shows the cross section of the sample with a borehole with a notch. If tensile failure is assumed, the fracturing pressure will be affected to some extent by the shape of bore holes and the radial crack will appear from the point of the notch. However, the experimental result indicates that the shape of borehole does not have any effect on the hydraulic fracturing pressure and in some cases even the direction of the cracks were different from the direction of the notch. Figure 13 shows a photograph of a sample after fracture initiation.

This behavior of the sample due to injecting water into the borehole might be another proof that initiation of hydraulic fracturing in cohesive soils can be considered by shear failure criteria.

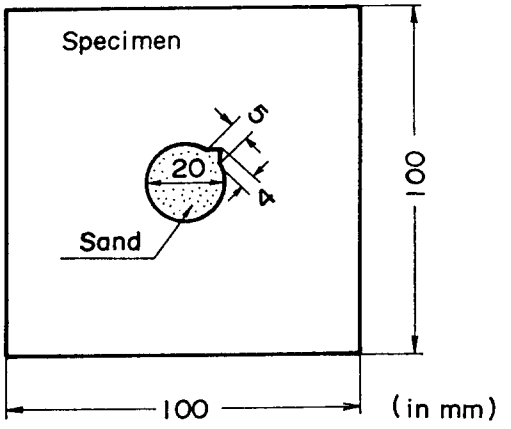

Fig. 12. Cross section of the sample with notch near the borehole

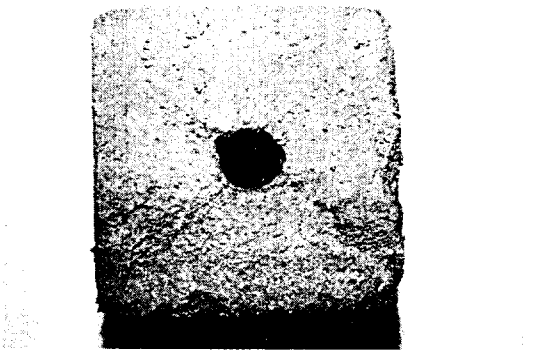

Fig. 13. Photograph of a specimen with notch after fracturing

EFFECT OF GROUND WATER

Let us consider the case of a portion of a bore hole located below the ground water table. In this case, pore water pressure has the value equal to a hydrostatic pressure U_0 throughout the sample and the excess pore pressure is added from inside the bore hole by the pressure P_f. In the cases in which hydrostatic pressure u_0 exists in the sample, a seepage condition through the specimen changes. In this condition pore pressure is increased uniformly from the inside to the outside of the specimen by the pressure u_0, therefore Eq. (26) becomes in the general form of:

$$P_f - u_0 = (1.5\sigma_3 - 0.5\sigma_1 - u_0)(1 + \sin\phi_u) + 2c_u \cos\phi_u. \quad (30)$$

Hydraulic fracturing initiation in the core of an earth dam in which residual pore pressure after construction or resulting pore pressure from the seepage of reservoir water exists can be analyzed by Eq. (30).

CONCLUSIONS

Two dimensional hydraulic fracturing criteria in cohesive soils was studied and the effects of principal stresses on the hydraulic fracturing pressure were examined by fracturing tests on cubical specimen. Fairly good agreement was obtained for the experimental values and predicted ones from Eq. (25).

The general form of the fracturing pressure was considered to be expressed by Eq. (30). The magnitude of maximum principal stress will have great effect on the hydraulic fracturing pressure. As the maximum principal stress increases, the hydraulic fracturing pressure will decrease.

The direction of the fractures are perpendicular to the minor principal stress plane and in the case of isotropic lateral pressure the fracture can initiate in any direction.

The shape of borehole does not have any effect on the hydraulic fracturing pressure and this suggests also shear failure of soil near the borehole.

NOTATION

a: internal radius of specimen
b: external radius of specimen
c_u: cohesion of soil in UU conditions
P_f: hydraulic fracturing pressure
q_u: unconfined compression strength
u: pore water pressure
u_0: excess pore water pressure
θ: direction angle
σ_h: confining pressure
σ_r, σ_{r1}, σ_{r2}, σ_{r3}: total radial stress
σ_θ, $\sigma_{\theta 1}$, $\sigma_{\theta 2}$, $\sigma_{\theta 3}$: total circumferential stress
σ_1: total maximum principal stress
σ_2: total intermediate principal stress
σ_3: total minimum principal stress
σ_r': effective radial stress
σ_u': effective circumferential stress
$\tau_{r\theta}$, $\tau_{r\theta 1}$, $\tau_{r\theta 2}$, $\tau_{r\theta 3}$: shear stress
ϕ_u: angle of internal friction of soil in UU conditions

REFERENCES

1) Bjerrum, L. and Andersen, K. H. (1972): "In situ measurements of lateral pressures in clay," Proceedings of the 5th European Conference on Soil Mechanics and Foundation Engineering, Madrid, Spain, Vol. 1, pp. 11-20.
2) Bjerrum, L., Nash, J. K. T. L., Kenard, R. M. and Gibson, R. E. (1974): "Hydraulic fracturing in field permeability testing," Geotechnique, London, England, Vol. 22, No. 2, pp. 319-332.
3) Fukushima, S. (1986): "Hydraulic fracturing criterion in the core of fill dams," Report of Fujita Kogyo Technical Institute, No. 22, pp. 131-136.
4) Independent Panel of Experts and Another of Top Dam Designers in Federal Agencies (1977): "Teton Dam failure," Civil Engineering, ASCE, pp. 56-61.
5) Independent Panel to Review Cause of Teton Dam Failure (1976): "Report to United States department of the interior and the State of Idaho on failure of Teton Dam," United States Bureau of Reclamation, Denver, Colo.
6) Jaworski, G. W., Duncan, J. M. and Seed, H. B. (1981): "Laboratory study of hydraulic fracturing," Journal of the Geotechnical Engineering Division, ASCE, pp. 713-732.

7) Kjaernsli, B. and Torblaa, I. (1968): "Leakage through horizontal cracks in the core of Hyttejuvet dam," Publication No. 80, Norwegian Geotechnical Institute, Oslo, Norway.
8) Komak Panah, A. and Yanagisawa, E. (1989): "Laboratory studies on hydraulic fracturing criteria in soil," Journal of the Soils and Foundations, Japanese Society of Soil Mechanics and Foundation Engineering, Vol. 29, No. 4, pp. 14-22.
9) Mori, A. and Tamura, M. (1987): "Hydrofracturing pressure of cohesive soils," Journal of the Soils and Foundations, Japanese Society of Soil Mechanics and Foundation Engineering, Vol. 27, No. 1, pp. 14-22.
10) Sherard, J. L. (1986): "Hydraulic fracturing in embankment dams," Journal of the Geotechnical Engineering Division, ASCE, Vol. 112, No. 10, pp. 905-927.
11) Vaughan, P. R. (1971): "The use of hydraulic fracturing tests to detect crack formation in embankment dam cores," Interim Report, Department of Civil Engineering, Imperial College, London, England.
12) Vaughan, P. R., Kluth, D. J., Leonard, M. W. and Pradowa, H. H. M. (1970): "Cracking and erosion of the rolled clay core of Balderhead dam and the remedial works adopted for its repair," Proceedings, 10th International Congress on Large Dams, Vol. 3, pp. 73-93.
13) Timoshenko, S. and Goodier, J. N. (1951): Theory of Elasticity, McGraw-Hill, pp. 78-81.